A magma "traffic jam" between lithosphere and asthenosphere

Along the axial zone of mid-ocean ridges (MOR), the asthenospheric mantle rises in response to the diverging motion of the oceanic lithosphere and experiences decompression melting. Depending on the volatile content and temperature of the upper mantle, peridotite partial melting initiates at depths of about 80 to 130 km. The resulting basaltic magmas are buoyant and mobile, percolating upward to form the crust, and leaving a refractory residuum that forms the oceanic lithosphere.

Structural changes in basaltic magmas with pressure (or depth) play a central role in the control of melting and magma mobility. Density measurements of basaltic magmas have thus far been carried out by the sink-float method [1]. Here, we apply X-ray absorption [2,3], an alternative method that enables the determination of liquid density under desired conditions. Furthermore, we use *in situ* falling-sphere viscometry and *in situ* X-ray diffraction [4,5] to measure magma viscosity and magma structure, respectively. The resulting complete and detailed dataset allows us to examine pressure-dependent changes in magma density, viscosity, and structure in unprecedented detail.

X-ray absorption measurements were performed up to 4.5 GPa and 2000 K at beamline **BL22XU**. We find that the density of basaltic magmas increases rapidly at pressures of ~4 GPa (Fig. 1(a)). Such rapid densification is consistent with previous studies on quenched aluminosilicate melts, which showed that Al coordination number increase rapidly between 3 and 5 GPa.

We further conducted *in situ* viscosity measurements by the falling-sphere method with X-ray radiography at beamline **BL04B1**. For basaltic magma, the isothermal viscosity first decreases and then increases with pressure. Viscosity minima are clearly discernible, both along the 1900 and 2000 K isotherms (Fig. 1(b)). The pressure of the viscosity minimum further coincides with that of rapid densification, suggesting that both are related to the same pressure-induced structural changes in the basaltic magma.

In order to clarify the nature of the structural changes, we performed X-ray diffraction experiments from 1.9 to 5.5 GPa at 1800 to 2000 K at beamline BL04B1. The X-ray diffraction interference functions, *Qi(Q)*, and its Fourier transform *G(r)*, i.e., the radial distribution function, are determined. The first peak at r = 1.6-1.7 Å in *G(r)* corresponds to the average T-O bond length, i.e., the length between tetrahedrally coordinated cations (T = Si^{4+}, Al^{3+}) and oxygen.

The T-O bond length is a characteristic parameter of the network structure of magmas. Figure 1(c) shows the T-O length of basaltic magma as a function of pressure, along with those of $MgSiO_3$ and $CaSiO_3$ melts, and corundum. No experimental data for the structure of basaltic magma at ambient pressure are available as a benchmark. For reference, we use the T-O length of anorthite melt at zero pressure. The T-O bond length in basaltic magma at ambient pressure may be shorter than that of anorthite melt because of the smaller Al_2O_3 content. We find that, for basaltic melt, the T-O length decreases between 1.9 and 4.3 GPa, and then increases between 4.3 and 5.5 GPa. Only the initial decrease is consistent with the simple compression of magma. As the T-O lengths in TO_6 octahedrons are generally longer than those in TO_4 tetrahedrons, the extension of the T-O length at high pressures is consistent with an increase in cation coordination. Between 4 and 6 GPa, the increase in Al^{3+} coordination is generally more extensive than that in

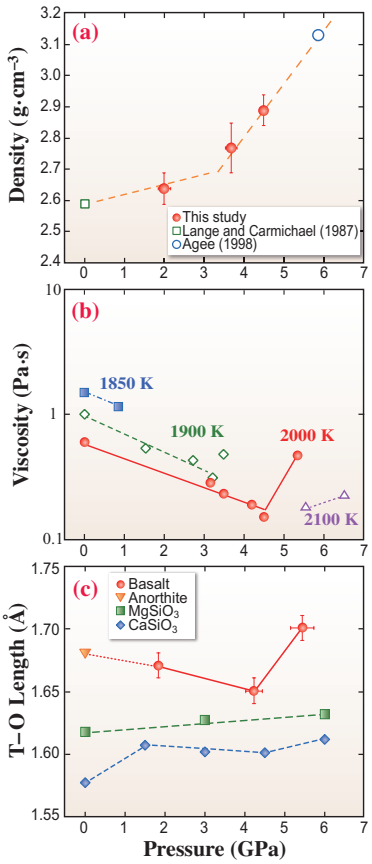

Fig. 1. Results of the experimental study. **(a)** Density of basaltic magma as a function of pressure at 2000 K. Anomalous densification occurs between 4 and 6 GPa. **(b)** Viscosity of basaltic magma at high pressure and temperature. **(c)** Pressure dependence of the T-O bond length of basaltic magma from this study, and other silicate melts from previous studies.

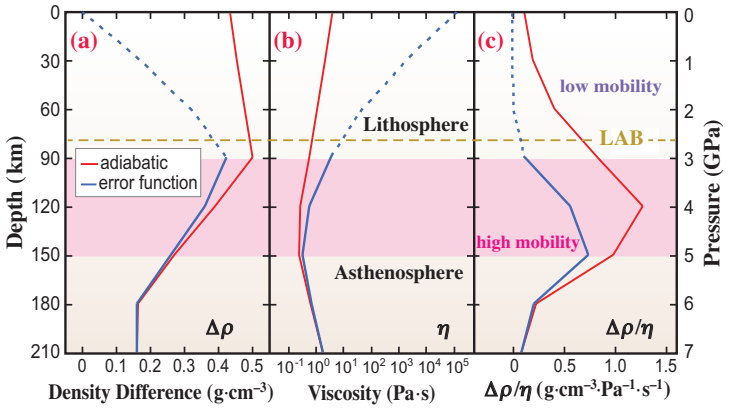

Fig. 2. Magma properties and mobility as a function of depth. **(a)** Density difference between basaltic magma and olivine ($\Delta\rho$) as a function of depth (and pressure). The red and blue lines are based on an adiabatic temperature gradient, and a realistic error-function temperature profile for mature oceanic lithosphere, respectively. The potential temperature is 1623 K. Pink shading highlights the depth range with anomalous physical properties of basaltic melts owing to the structural transition in Al coordination. **(b)** Viscosity (η) of basaltic magma along the same two profiles. Hypothetical subsolidus density and viscosity profiles are shown by dashed lines. **(c)** Mobility $\Delta\rho/\eta$ of basaltic magma along the same two profiles.

Si^{4+} coordination. Therefore, the rapid density increase of basaltic magma at these pressures is attributed to an increase in Al^{3+} coordination. This behavior is unique compared with other silicic melts: T-O lengths have been reported to only modestly increase with pressure for $MgSiO_3$ and $CaSiO_3$ melts (Fig. 1(c)).

Gravity-driven separation of buoyant magma from partially molten rock is proportional to the "hydrostatic magma mobility" (defined as $\Delta\rho/\eta$) in addition to the permeability. Here, η is the melt viscosity, and $\Delta\rho$ is the density difference between the magma and the surrounding solid rock (for which we take olivine Fo_{90} as representative). Figure 2(a) shows that, for any plausible choice of geotherm, $\Delta\rho$ decreases rapidly from 100 to 180 km depth (i.e., ~3.5 to ~6 GPa). This transition is caused by a coordination change of Al in the melt with an unusually large compressibility of almost five times higher than usual above and below this depth range. Also, $\Delta\rho$ slightly decreases from a depth of ~100 km to the surface (Fig. 2(a)). This slight decrease in $\Delta\rho$ is a conservative estimate as we do not consider the effects of the successive removal of garnet and clinopyroxene, nor those of an increase in Mg# (in olivine) in the residual MOR melting column (i.e., the oceanic lithosphere). The resulting maximum $\Delta\rho$ at 3-4 GPa, in combination with minimum η at 4-5 GPa (Fig. 2(b)), results in a peak in magma mobility at ~120-150 km depth in the Earth's mantle (Fig. 2(c)).

The peak in melt mobility at ~120-150 km depth carries important implications for the nature of Earth's shallow mantle. The decreased mobility of melt as magma ascends from a partially molten asthenosphere gives rise to the tendency of excess melt accumulation at 80-100 km depth (Fig. 3). Unless vertical dikes or channels form in the lithosphere that would otherwise allow the melts to escape, magma generated at depth would accumulate atop the asthenosphere. Indeed, a recent magnetotelluric study suggests such a scenario beneath the edge of the Cocos plate. Excessive melt accumulation at these depths may also lead to rheological weakening, enhanced shear deformation, and the formation of sub-horizontal melt bands that would further decrease vertical melt mobility. However, this excess magma may also be cooled by heat conduction to the overlying lithosphere, which would cause it to freeze, further restricting permeability and possibly giving rise to the formation of an extensive network of basaltic sills at the base of the lithosphere. Excess melt accumulation at 80-100 km depth may help explain the origin of the seismically observed Gutenberg discontinuity, as well as its geographical correlation with features suggestive of recent partial melting of the mantle.

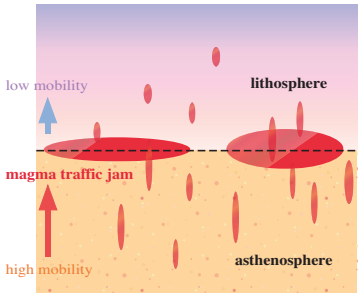

Fig. 3. Schematic illustration of the lithosphere and asthenosphere boundary (LAB). Magma mobility is faster between 120 km and 150 km, causing relative magma depletion. The LAB at around 80 km depth can be a zone of excessive melt accumulation, since it can be fluxed at higher rates from below where mobility is higher, but is removed at much slower rate above where mobility is lower.

Tatsuya Sakamaki

Dept. of Earth and Planetary Materials Science,
Tohoku University

E-mail: sakamaki@m.tohoku.ac.jp

References

[1] T. Sakamaki *et al.*: Nature **439** (2006) 192.
[2] T. Sakamaki *et al.*: Earth Planet. Sci. Lett. **287** (2009) 293.
[3] T. Sakamaki *et al.*: Am. Mineral. **95** (2010) 144.
[4] T. Sakamaki *et al.*: J. Appl. Phys. **111** (2012) 112623.
[5] *T. Sakamaki, A. Suzuki, E. Ohtani, H. Terasaki, S. Urakawa, Y. Katayama, K. Funakoshi, Y. Wang, J. Hernlund, M. Ballmer: Nat. Geosci.* ***6*** *(2013) 1041.*